

Apparent teleportation of indistinguishable particles

M. Gazdzicki,¹ D. Kikoła,² I. Pidhurskyi,^{1,3} and L. Tinti¹

¹*Jan Kochanowski University, Kielce, Poland*

²*Warsaw University of Technology, Warsaw, Poland*

³*European Organization for Nuclear Research, CERN, Geneva, Switzerland*

Abstract

Teleportation, introduced in science fiction literature, is an instantaneous change of the position of a macroscopic object. Two teleportation-like phenomena were predicted by quantum mechanics: quantum teleportation and, recently, quantum particle teleportation. The former is investigated experimentally and has applications in quantum communication and computing.

Here, we introduced the third teleportation-like phenomenon—apparent teleportation. It seems to be a natural consequence of the Standard Model’s indistinguishable elementary particles and antiparticles. We give an example of a process leading to the apparent teleportation within a 1+1D toy model of particle space-time evolution. It utilizes the local transport of particles and antiparticles and the local creation and annihilation of particle-antiparticle pairs. Furthermore, we suggest a method to observe the apparent teleportation in nucleus-nucleus collisions at properly selected collision energies. The method requires the measurement of correlations between momenta of charm and anticharm hadrons in collisions with a single $c\bar{c}$ pair being produced. The ultimate prediction following the apparent teleportation hypothesis is the uncorrelated emission of charm and anticharm hadrons. It can be tested by contemporary experiments.

Observing the apparent teleportation would uncover the basic transport properties of indistinguishable particles. In particular, the apparent teleportation may explain the rapid thermalisation of the system created in collisions of two atomic nuclei and the quark-gluon plasma hadronisation paradox. Theoretical and experimental efforts are needed to observe the apparent teleportation processes and study their properties.

Teleportation [1] is rooted in science fiction. It describes the ability of macroscopic objects, for example, humans, to reappear at some distant location without traversing space. Thus, the speed of light does not restrict the possibility of changing our location in space. Needless to say, this also concerns signals. Details depend on the science fiction setup.

Quantum teleportation [2] is the standard quantum physics phenomenon - transferring quantum-state properties over arbitrarily large distances in no time. In quantum teleportation, conditional probabilities of measurement outcomes reappear at a distant location using the entanglement of two particles. There is neither a super-luminal transfer of conserved quantities nor super-luminal signalling. The quantum teleportation is measured in numerous experiments [3–6].

Quantum particle teleportation [7] is an instantaneous transfer of a single particle over a large distance predicted by standard quantum mechanics. The phenomenon appears for particles in a potential. It is induced by frequently monitoring if the particle is at rest (a peculiar quantum Zeno dynamics [8–10]). Quantum particle teleportation has the properties of "science fiction" teleportation, allowing for the reappearance of conserved quantities and signalling. It was predicted in 2023 and has not yet been tested experimentally.

Apparent teleportation (AT) is a concept introduced here. It is defined as the time evolution of a system of indistinguishable particles that cannot be mimicked by distinguishable particles moving with luminal or subluminal velocities. Of course, when referring to distinguishable particles mimicking indistinguishable ones, we assume the observer is blind to particle labels. The apparent teleportation seemingly requires superluminal velocities of particles. This illusion results from particle trajectories and velocities being defined for distinguishable particles but undefined for indistinguishable ones.

I. RESULTS

Elementary particles and antiparticles of the Standard Model are indistinguishable bosons and fermions. Objects composed of many indistinguishable elementary particles and antiparticles are close-to-unique and thus can be approximately treated as distinguishable ones [11]. Classical physics is rooted in our daily experience within the world of macroscopic distinguish-

able humans and other objects. In particular, it is well established that they can move only with velocities smaller than the speed of light. However, applying time evolution limits of distinguishable objects to indistinguishable particles and antiparticles imposes human-centered experience on a fundamentally different quantum world. In particular, the problem is obvious if these limits are given in quantities undefined for indistinguishable particles and antiparticles, like particle velocity. In this sense, the apparent teleportation is the natural property of models postulating the indistinguishability of elementary particles and antiparticles.

In the following, we give a simple example of a model predicting the apparent teleportation. It is a toy model of particle-antiparticle creation, annihilation, and transport. Secondly, we present an idea of experimentally observing the apparent teleportation in collisions of two nuclei.

A. Toy model of apparent teleportation

Cell Model is a dynamical model based on the 1+1D discrete-time Markov chain framework [12, 13]. Space is assumed to be a vector of V discrete cells (v_1, v_2, \dots, v_V) arranged in a ring. At the given time t , the system microstate is fully defined by a distribution of particles and antiparticles in cells. The system's evolution in time is assumed to be discrete, and the time steps are numbered by t . During evolution, transitions between the systems' microstates occur. The transition probability from a microstate X at t to a microstate Y at $t + 1$ depends only on the microstate X - the basic assumption of Markov's chains.

For this paper, we consider three types of reactions changing the system's microstates:

- particle-antiparticle creation in a single cell,
- particle-antiparticle annihilation in a single cell and,
- redistribution of particles and antiparticles between cells.

The first two reactions change the number of particles and antiparticles, whereas the third only changes their distribution in cells. The difference between particle and antiparticle numbers of a given type is conserved in the whole system. This is the only conservation law imposed on the system. In relation to quantum mechanics, the time steps are considered times at which a

measurement of (anti-)particles' positions in space is performed, and the uncertainty principle gives the size of cells in space.

In summary, the distribution of particles and antiparticles in cells differs at different time steps. These changes can be due to particle-antiparticle creation-annihilation reactions and particle and antiparticle redistribution. Now, we postulate that only changes obeying the *transport locality* are allowed during the redistribution. For distinguishable particles, the transport-locality requirement reduces to a requirement of each particle moving by no more than Δ cells. In physics, this corresponds to particle velocities, which are limited by the speed of light in the vacuum.

For indistinguishable particles, the particle's trajectories and velocities are undefined. Thus, the transport locality condition for distinguishable particles does not apply to indistinguishable ones. The condition for indistinguishable particles and antiparticles is unknown, and experiments are needed to uncover it.

Here, we assume that the transport locality condition introduced for a conserved charge without considering particle-antiparticle creation and annihilation processes [13] (see below) is valid separately for redistributions of indistinguishable particles and antiparticles. It implies the following. During a single time step, the particle (antiparticle) number in any interval of cells cannot be transported beyond an interval by Δ cells longer on the left and right. Moreover, it cannot be squeezed to an interval by Δ cells shorter on the left and right. The condition means that only those redistributions of particles (antiparticles) that can be mimicked by distinguishable particles (antiparticles) are possible. The condition is given by two transport-locality inequalities [13]:

$$\begin{aligned} \sum_{j=i}^{i+k} n_j^X &\leq \sum_{l=i-\Delta}^{i+k+\Delta} n_l^Y, \\ \sum_{l=i}^{i+k} n_l^Y &\leq \sum_{j=i-\Delta}^{i+k+\Delta} n_j^X, \end{aligned} \tag{1}$$

where $k = 0, 1, \dots$ and n_j^X, n_l^Y are particle numbers in cells j, l of X and Y microstates, respectively. If the (anti)particle number in a single cell is unlimited, the inequalities concern bosons; if the number is limited to 0 and 1, they concern fermions.

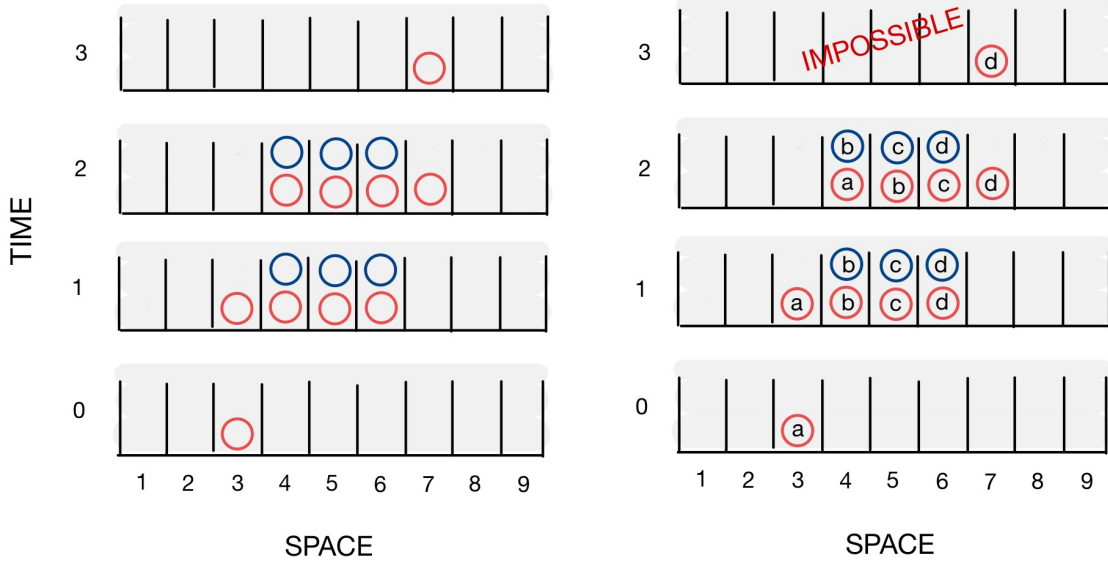


Figure 1: The simple setup illustrates the apparent teleportation of indistinguishable particles within the Cell Model. The maximum distance a distinguishable particle and antiparticle can move during a time step is set to $\Delta = 1$. Three types of transitions, pair creation, local transport and pair annihilation, are possible. *Left:* The example process with indistinguishable particles starting from a single particle in cell three at $t = 0$ and ending in a single particle in cell seven at $t = 3$. *Right:* Unsuccessful attempt to mimic the process by distinguishable particles. Three pairs of particles and antiparticles with identical labels appear at $t = 1$. Particles are shifted by one cell to the right at $t = 2$. In particular, the particle 'd' appears in cell seven. The particle number distributions for indistinguishable and distinguishable particles are identical at $t = 0$, 1 and 2. The pair annihilation reactions in cells 4, 5 and 6 are impossible during the third step because cells contain particles and antiparticles with different labels. For example, cell 4 contains particle 'a' and antiparticle 'b' at $t = 2$. See the text for more details.

Apparent teleportation within Cell Model is illustrated in Fig. 1. An example of the system's time evolution with $V = 9$ cells and periodic boundary conditions is shown. Cells contain "background" particles carrying total energy depicted by the grey band. Particles and antiparticles of interest (for example, c and \bar{c} quarks, see below) are depicted by red and blue circles, respectively. For simplicity, we assume that the speed of light results in $\Delta = 1$. The

difference between the total number of particles and antiparticles is assumed to be conserved.

The case of indistinguishable particles and antiparticles is presented in the left plot of Fig. 1. We postulate that only one particle exists at $t = 0$, and it is in cell 3. Three pairs of particles and antiparticles appear in cells 4, 5 and 6 at $t = 1$. At $t = 2$, the particle number distribution is shifted by one cell to the right by the transport-local transition with $\Delta = 1$. This is allowed by the transport-locality inequalities (1). Then, at $t = 3$, particle-antiparticle pairs annihilate, leaving a single particle in cell seven.

The right plot of Fig. 1 shows an unsuccessful attempt to mimic the above process using distinguishable particles. In the example presented here, they are labeled by the letters 'a', 'b', 'c', and 'd'. Similarly, antiparticles have unique labels. Only creating a particle and an antiparticle with identical labels is possible. Similarly, only a particle and an antiparticle with identical labels can annihilate.

For the label-blind observer, the particle and antiparticle number distributions of indistinguishable and distinguishable particles are identical at $t = 0, 1$, and 2. But the similarity breaks at $t = 3$. This is because annihilating particles and antiparticles with different labels is impossible. Of course, distinguishable particles can mimic the process depicted in the left plot if the transport-locality requirement is lifted. Particle 'a' can be 'teleported' by four cells in three-step steps from cell 3 to 7.

The example construction of the process shown in Fig. 1 can be easily generalized, allowing for an arbitrary redistribution of indistinguishable boson-like particles and antiparticles in three-time steps. This includes apparent teleportations - the processes which seemingly violate the speed of light limit. Their rate will increase with the increasing rate of creation and annihilation reactions and thus with energy density. Following the quantum mechanics, the creation and annihilation of virtual (disobeying conservation laws for a short time) particles and antiparticles is also possible.

We note that the microscopic mechanism of the apparent teleportation illustrated in Fig. 5 (*left*) cannot be used for superluminal signalling. An observer in cell seven detecting a particle at $t = 3$ cannot be sure it is caused by injecting a particle at $t = 0$ in cell three. For example, it could be due to the creation of particle and antiparticle pair in cell six independently of events in cell three and then a particle appearing in cell seven.

The probability of a given process depends on the dynamics. One can speculate that at sufficiently high energy densities, the system of indistinguishable particles approaches maximum symmetry (the microstate symmetry [13]), and all processes have the same probability. This would imply that the system is "born in equilibrium" [14] - the probability of any microstate appearing at any time is equal. The apparent teleportation also seem to explain the quark-gluon paradox formulated in Ref. [15]. The transition of large volume quark-gluon plasma created in collisions of two atomic nuclei (see below for details) to Colorless hadrons require "teleportation" of colour charge to assure local colour neutrality. Quarks and gluons are indistinguishable particles. Thus, the apparent teleportation can serve as the physical mechanism of the "teleportation".

The above discussion suggests that the experimental search for apparent teleportation is the most promising at high energy densities, where the particle and antiparticle density is high, and their creation and annihilation reactions are frequent.

B. Observing apparent teleportation

System of quarks and gluons created in nucleus-nucleus collisions at high energies is the highest energy density system ($\epsilon > 1 \text{ GeV}/\text{fm}^3 \approx 1.6 \cdot 10^{35} \text{ J}/\text{m}^3$) created under conditions controlled in the laboratory [16]. Its equilibrium state is called quark-gluon plasma (QGP) [17]. Its total charge of strong interactions, colour, is zero. The plasma expands and cools down, and the transition to colour-neutral hadrons - small bags of quarks and gluons - occurs at the hadronisation (transition) temperature $T_H \approx 150 \text{ MeV}$ [18].

Six types of quarks (fermions) u, d, s, c, t and b and the corresponding antiquarks and the eight types of gluons (bosons) can be created during the collision. Particles and antiparticles of a given type are indistinguishable. Massless gluons and light u and d quarks and antiquarks are the most abundant. Production of other quarks is suppressed even at the top collision energies of the CERN LHC [19]. The threshold for the QGP creation in heavy-ion collisions is located at $\sqrt{s_{NN}} \approx 10 \text{ GeV}/c$ [20, 21], for review see also Refs. [22, 23]. The fixed target experiments at the CERN SPS measure heavy-ion collisions in the energy range $\sqrt{s_{NN}} \approx 5 - 20 \text{ GeV}/c$. At

the top SPS energy, just above the QGP threshold energy, the mean number of light quarks and gluons produced in central collisions of two lead nuclei is on the order of 1000 [24]. The corresponding numbers for strange and charm quarks are ≈ 100 [24] and ≈ 1 [25], respectively.

The local creation and annihilation of c and \bar{c} pairs mean that the energy and momentum scale of the interaction determines c - \bar{c} space-time separation via the uncertainty principle. The scale ranges between:

- the hard-scattering scale of the isolated reaction, $\hbar c/(2m_c) \approx 0.1$ fm, with $m_c \approx 1.3$ GeV being the charm quark mass, and
- the thermal scale of the reaction in the dense quark-gluon plasma, $\hbar c/T \approx 1$ fm, with $T \approx 0.2$ GeV being the quark-gluon plasma temperature just above the transition (hadronisation) temperature.

The spatial extent and lifetime of the system created in central Pb+Pb collisions are on the order of approximately 10 fm, the diameter of the lead nucleus. It is much larger than the space-time cell in which local creation and annihilation of c and \bar{c} quarks occur. It opens the possibility of observing the apparent teleportation in the collisions.

Observing apparent teleportation in heavy-ion collisions is likely to be a challenging task. This is due to two reasons:

- The experimental challenge: We cannot measure the location in the space of a single charm quark created in a collision at two different times. Hence, the simple setup presented in Fig. 1 cannot be used for observing the apparent teleportation.
- The theoretical challenge: Quantum Chromodynamics, the theory of strong interactions, does not provide quantitative predictions for multi-particle correlations in heavy-ion collisions; for further discussion, see Ref. [26].

However, with the help of well-established heavy-ion models, it may be possible to provide experimental evidence of the apparent teleportation by measuring momentum correlations between c and \bar{c} quarks. The idea is rooted in our previous paper [26], which suggested the use of momentum correlations of charm-anticharm hadrons to extract information on spatial

correlations of c and \bar{c} quarks at hadronisation. The paper reviews the experimental results on charm hadron correlations and collective flow. It also discusses the importance of having collisions with no more than one $c\bar{c}$ pair created. We note that the requirement of a single $c\bar{c}$ pair in a collision can be reconciled with the example of the apparent teleportation mechanism presented in Sec. I A, assuming that virtual $c\bar{c}$ pairs are produced at a sufficiently high rate. Below, we detail the idea.

The standard model of heavy-ion collisions at high energies describes the collision as follows.

- (a) Initial stage: a high-density quark-gluon plasma is created.
- (b) Expansion stage: the plasma expands [27], cooling down to the hadronisation temperature ($T_H \approx 150$ MeV in the local frame of the flowing matter). This stage is modelled using relativistic hydrodynamics [16].
- (c) Hadronisation stage: the plasma is converted into hadrons and resonances following statistical rules [28, 29] applied in the rest frame of a plasma fluid element. As a result, hadron momenta are determined by their flow acquired during the expansion stage and by the hadronisation (a local statistical process).
- (d) Free-streaming stage: resonances decay, and non-interacting hadrons freely stream in a vacuum to a detector.

We illustrate the idea of observing the apparent teleportation with the help of the schematic 1+1D model of the collisions sketched in Fig. 2. For simplicity, we assume that the initial stage is created at $t = 0$ and extends in space from $-R$ to R . The hadronisation occurs at $t = R$; at this stage, the system extends from $-2R$ to $2R$. For simplicity, we neglect the finite size of the space-time cell of the local $c\bar{c}$ pair creation. In the middle and bottom plots, two examples of the hadronisation points of a single $c\bar{c}$ pair created in the collision are depicted as r_c and $r_{\bar{c}}$. The plots also show the past light cones of the charm and anticharm quarks (the blue and red areas).

Let us assume the c and \bar{c} quarks were created in the same space-time point within the collision light cone and moved to hadronisation as distinguishable particles with subluminal

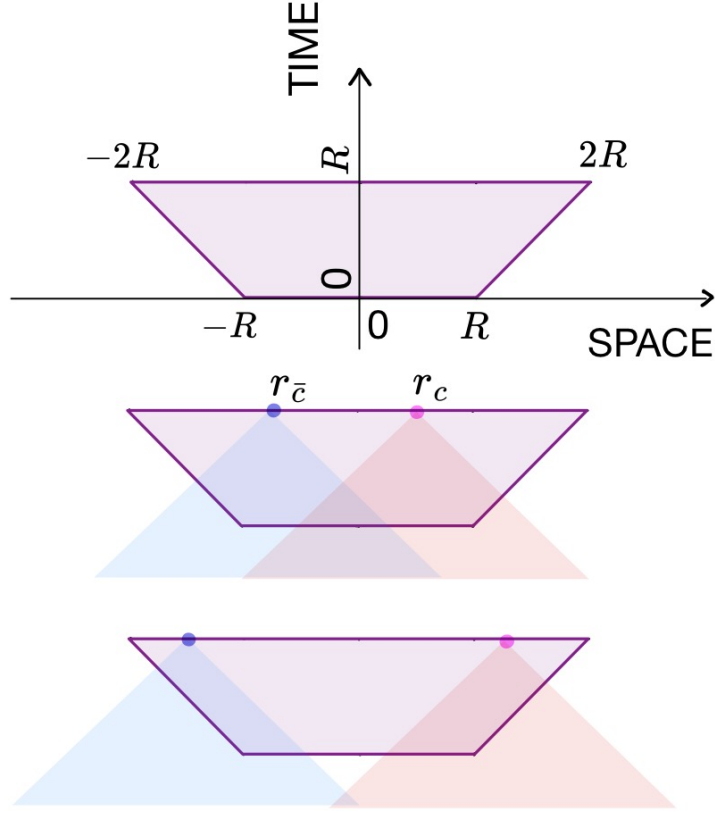


Figure 2: The simplest illustration of observing the apparent teleportation in heavy-ion collisions at high energies using a single pair of c and \bar{c} quarks. The top plot shows the space-time (1+1D) evolution of the quark-gluon plasma created at $t = 0$ in the spatial region from $-R$ to R . The hadronisation is assumed to occur at $t = R$ when the system extends from $-2R$ to $2R$. The middle plot shows an example of the positions of the c and \bar{c} quarks at hadronisation, denoted as r_c and $r_{\bar{c}}$, respectively. In this example, the past light cones of the quarks overlap within the collision light cone. This overlap is required for the subluminal movement of distinguishable c and \bar{c} quarks created at a common space-time point. We refer to this as the local indistinguishability condition (LD condition). The bottom plot depicts the positions of the c and \bar{c} quarks, which can only be explained by the apparent teleportation.

velocities. In this case, the creation point has to be located inside the overlap between the collision light cone and the past-light cones of c and \bar{c} quarks - the local-distinguishable (LD)

condition. The $c\bar{c}$ pair depicted in the middle plot of Fig. 2 fulfils the requirement, but the pair depicted in the bottom plot does not. The latter implies that the process was not local-distinguishable, and one needs the apparent teleportation to explain it.

Within the example shown in Fig. 2, the LD condition reads $|r_c - r_{\bar{c}}| \leq 2R$. The apparent teleportation is required if the LD condition is violated, $|r_c - r_{\bar{c}}| > 2R$. The positions of quarks at hadronisation are not measured. Instead, experiments measure velocities (momenta) of charm hadrons in the free-streaming stage. We relate them in two steps: first, we introduce the correlation between the quark position and its flow velocity, and second, we unfold the flow velocity smearing due to the quark interactions with the medium and hadronisation.

Let us assume that the velocities of charm quarks at hadronisation are equal to the flow velocities of matter at the hadronisation points. For simplicity, we also assume that the flow velocity is proportional to the distance from the collision centre. From these assumptions, it follows that the apparent teleportation is required if $|\beta_c - \beta_{\bar{c}}| > 1$, where β_c and $\beta_{\bar{c}}$ are c and \bar{c} quark velocities scaled by the light velocity. The pairs which obey the complementary condition, $|\beta_c - \beta_{\bar{c}}| \leq 1$, may come either from LD or AT processes. Allowed processes leading to pairs with given β_c and $\beta_{\bar{c}}$ values are depicted in Fig. 3.

After the hadronisation stage, the carriers of the c and \bar{c} quarks are charm and anticharm hadrons. For simplicity, we assume these are D and \bar{D} mesons. The free-streaming velocities of these mesons, β_D and $\beta_{\bar{D}}$, are superpositions of the quark flow velocities ($\beta_c, \beta_{\bar{c}}$) and a stochastic, non-flow component. The non-flow component may arise from initial momenta of quarks, their diffusion in quark-gluon plasma, hadronisation, and following decay of resonances. In Methods, we illustrate the effect of the smearing by the stochastic uncorrelated processes. We show the calculation results within the 1+1D model with the Hubble-like initial and hadronisation hypersurfaces and uncorrelated smearing included. The predictions for the 1+3D model with the blast-wave hadronisation hypersurface are also presented in Methods.

Assuming that the stochastic components of D and \bar{D} are uncorrelated, the desired joint probability density function, $\rho(\beta_c, \beta_{\bar{c}})$, can be extracted from the measured $\rho(\beta_D, \beta_{\bar{D}})$ in an almost model-independent manner. The procedure is detailed in Ref. [26].

The initial c and \bar{c} momenta may be correlated due to energy-momentum conservation. Remnants of this correlation might persist throughout the transport process, leading to correlated

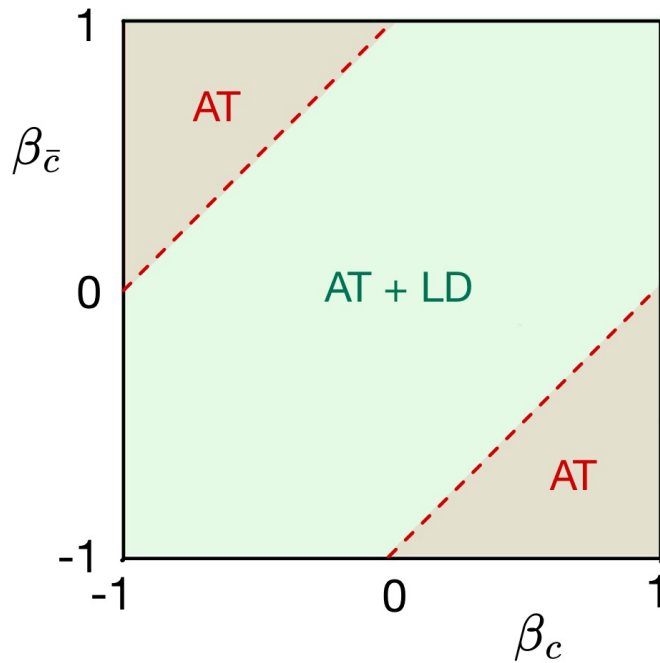


Figure 3: The simplest (1+1) D model of heavy-ion collisions and charm production explains the idea of observing apparent teleportation. Processes resulting in c and \bar{c} quarks at hadronisation with flow velocities β_c and $\beta_{\bar{c}}$ are depicted as AT - apparent teleportation and LD - local distinguishable. The corners cut by the red dashed lines are forbidden for the local distinguishable but allowed for the apparent teleportation processes.

non-flow components in the D and \bar{D} momenta. At collision energies where the creation of c and \bar{c} quarks occurs near the threshold—such that no more than one $c\bar{c}$ pair is produced per collision—it is reasonable to expect that the initial quark momenta are small. Consequently, the correlated non-flow component is likely to be negligibly small. A quantitative estimate of this effect lies beyond the scope of the present paper.

The apparent teleportation may render all transitions possible. One may speculate that at very high energy densities, the microstate-symmetric transition matrix [13] may govern the system's evolution. This implies that c and \bar{c} quarks, and consequently D and \bar{D} hadrons, are produced independently in space-time and momentum. The joint probability density function

$\rho(\beta_D, \beta_{\bar{D}})$ factorises as:

$$\rho(\beta_D, \beta_{\bar{D}}) = \rho(\beta_D) \cdot \rho(\beta_{\bar{D}}) , \quad (2)$$

and, in the general 1+3D case:

$$\rho(\mathbf{p}_D, \mathbf{p}_{\bar{D}}) = \rho(\mathbf{p}_D) \cdot \rho(\mathbf{p}_{\bar{D}}) , \quad (3)$$

where \mathbf{p}_D and $\mathbf{p}_{\bar{D}}$ are the momentum vectors of D and \bar{D} hadrons, respectively. Contemporary experiments can test this extreme prediction following the apparent teleportation hypothesis soon [26]. This requires measurements of sufficiently high statistics of charm and anticharm hadron pairs produced in individual collisions with a mean multiplicity of the pairs below one [26].

II. DISCUSSION

We argue that the apparent teleportation of indistinguishable particles naturally follows from the Standard Model postulate of elementary particles being indistinguishable. Thus, apparent teleportation is expected in many systems of indistinguishable particles and antiparticles.

The presented example of the apparent teleportation process suggests that the particle-antiparticle creation and annihilation reactions, real and virtual, are required for apparent teleportation—their rate increases with the system’s energy density. Thus, apparent teleportation is expected to be more popular in high-energy-density systems. It makes it difficult to observe experimentally. This is because the high-density systems created in laboratories typically have small spatial and temporal dimensions. Therefore, precisely measuring particle number distribution in short intervals may be challenging.

We provide an example of overcoming the problem of observing the apparent teleportation. It can be done by measuring momentum correlation of charm and anticharm hadrons produced in collisions of two sufficiently heavy atomic nuclei with only one pair of charm and anti-charm quarks created. Contemporary experiments can perform the measurement; however, interpreting results on apparent teleportation will depend on modelling the time evolution of the strongly interacting system. Other experimental setups should be considered, giving together evidence of the apparent teleportation of indistinguishable particles.

If it exists, the apparent teleportation may explain two puzzles about nuclear collisions at high energies: the fast equilibration of the created system of quarks and gluons and its fast hadronisation fulfilling the requirement of local colour neutrality.

Methods

1+1D Hubble-like model

Here, we present predictions for the apparent teleportation using a one-dimensional evolution with Hubble-like flow, including a simple model of hadronisation of heavy quarks. The calculations follow the approach we introduced in Ref. [26] for a spherically symmetric system.

The shape of the initial system is described by its initial hypersurface:

$$t^2 = z^2 + \tau_0^2, \quad (4)$$

where τ_0 is the initial proper time at which the system is formed, and z is the distance from the system's centre. The system then undergoes a Hubble-like expansion, and the hadronisation hypersurface is taken as

$$t^2 = z^2 + \tau_{\text{HAD}}^2, \quad (5)$$

where τ_{HAD} is the hadronisation proper time. The expanding matter is assumed to be in local equilibrium corresponding to temperatures T_0 and T_{HAD} at proper times τ_0 and τ_{HAD} , respectively. The matter density is assumed to be uniform along the hadronisation hypersurface, which is limited in z as $|z| < \tau_{\text{HAD}} + R_{\text{MAX}}$. In the following the parameters τ_{HAD} and R_{MAX} are fixed to 10 fm and 6 fm, being on the order of the Pb nucleus radius. Figure 4 shows a sketch illustrating the hypersurfaces and indicating its parameters.

For the Hubble-like flow, the energy conservation relates the initial parameters τ_0 and T_0 to the hadronisation parameters τ_{HAD} and T_{HAD} as:

$$\frac{\tau_0}{\tau_{\text{HAD}}} = 1 - \frac{3}{4} \ln \left(\frac{T_0}{T_{\text{HAD}}} \right). \quad (6)$$

The hadronisation temperature is set to the well-known value from the lattice QCD, 150 MeV [18]. The initial temperature T_0 has to be larger than the hadronisation one. Below, we present examples calculated for $T_0 = 200$ MeV and $T_0 = 300$ MeV. The latter value is close to the initial temperature given by the Fermi-Landau initial conditions [24] at the top energy CERN

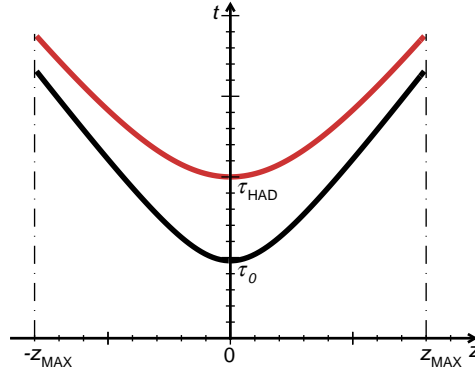


Figure 4: Sketch of the 1+1D Hubble-like model of the space-time evolution of the system created in lead-lead collisions. The black curve shows the initial hypersurface defined by the proper time τ_0 at which the system is formed and its expansion starts. The red curve presents the hadronisation hypersurface given by the τ_{HAD} parameter.

SPS. It can be considered as the upper limit of T_0 at SPS. The remaining parameter of the model τ_0 is calculated using Eq. 6. The velocity of the fluid element and (anti)charm quarks at the hadronisation is given by the Hubble flow assumption, $u = z/\tau_{\text{HAD}}$.

At the hadronisation, (anti)charm quarks are converted into (anti) D mesons. To model this process, the momentum of the (anti)charmed mesons at the fluid rest frame p'_D is drawn from the statistical-like distribution:

$$dN/dp'_D \propto p'^2_D \cdot e^{-\sqrt{m_D^2 + p'^2_D} / T_{\text{HAD}}}, \quad (7)$$

where we use mass of D^0 meson $m_D = 1.869$ GeV. Finally, the momentum p_D in the laboratory frame at hadronisation is calculated by boosting p'_D with the fluid-element velocity. To assess how the statistical hadronisation influences the expected signal of the apparent teleportation, we also considered a case with $p'_D = 0$, thus removing the effect of statistical smearing of the momentum of (anti)charm mesons.

Figure 5 shows two examples ($T_0 = 200$ MeV (a) and $T_0 = 300$ MeV (b)) of the hadronisation points of charm and anti-charm quarks requiring the apparent teleportation - the past light cones of c and \bar{c} quarks overlap only below the initial hypersurface. We notice that the larger T_0 is, the smaller the space for separating the apparent teleportation from the local-distinguishable processes. The apparent teleportation processes can be separated up to $T_0 \approx 400$ MeV within

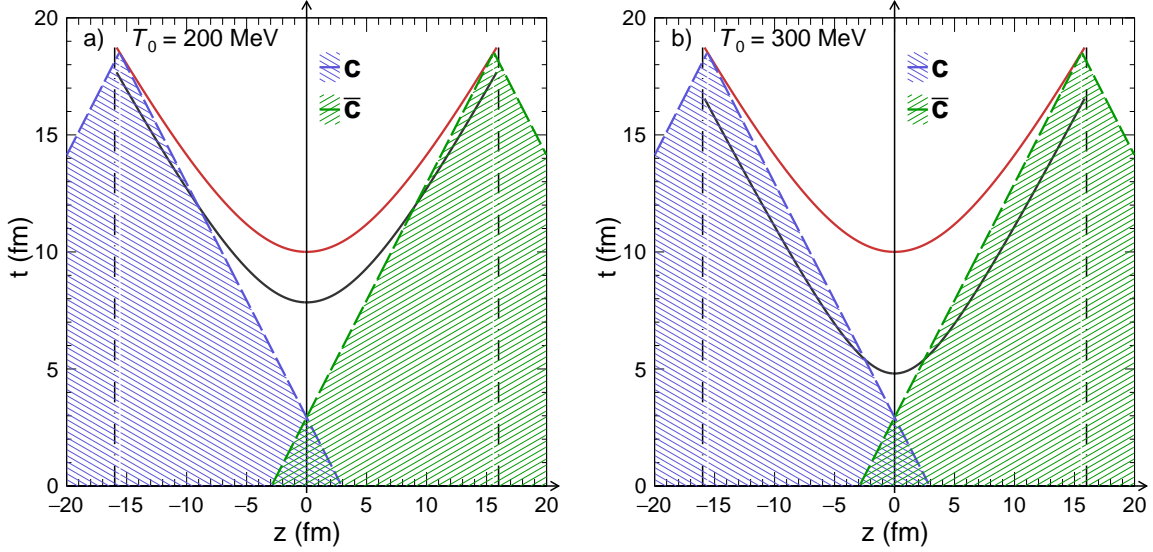


Figure 5: Examples of hadronisation points of c and \bar{c} quarks that can only result from the apparent hadronisation. The initial temperature is set to $T_0 = 200$ MeV (a) and $T_0 = 300$ MeV (b). The black lines indicate the initial hypersurface, and the hadronisation hypersurface is shown by red lines.

the model and for its parameters.

Figures 6 and 7 show the joint rapidity distributions of D and \bar{D} mesons for $\tau_{\text{HAD}} = 10$ fm for $T_0 = 200$ MeV and $T_0 = 300$ MeV, respectively. The space for separating the apparent teleportation is significantly larger for the lower value of T_0 . Including statistical hadronisation significantly smears the joint rapidity distributions. In this case, separating the apparent teleportation will require correcting the 2D distributions for the smearing as discussed in Ref. [26].

Our study shows that apparent teleportation can be observed in heavy-ion collisions at the SPS energy. The chance of success depends on the system's initial temperature and the hadronisation hypersurface.

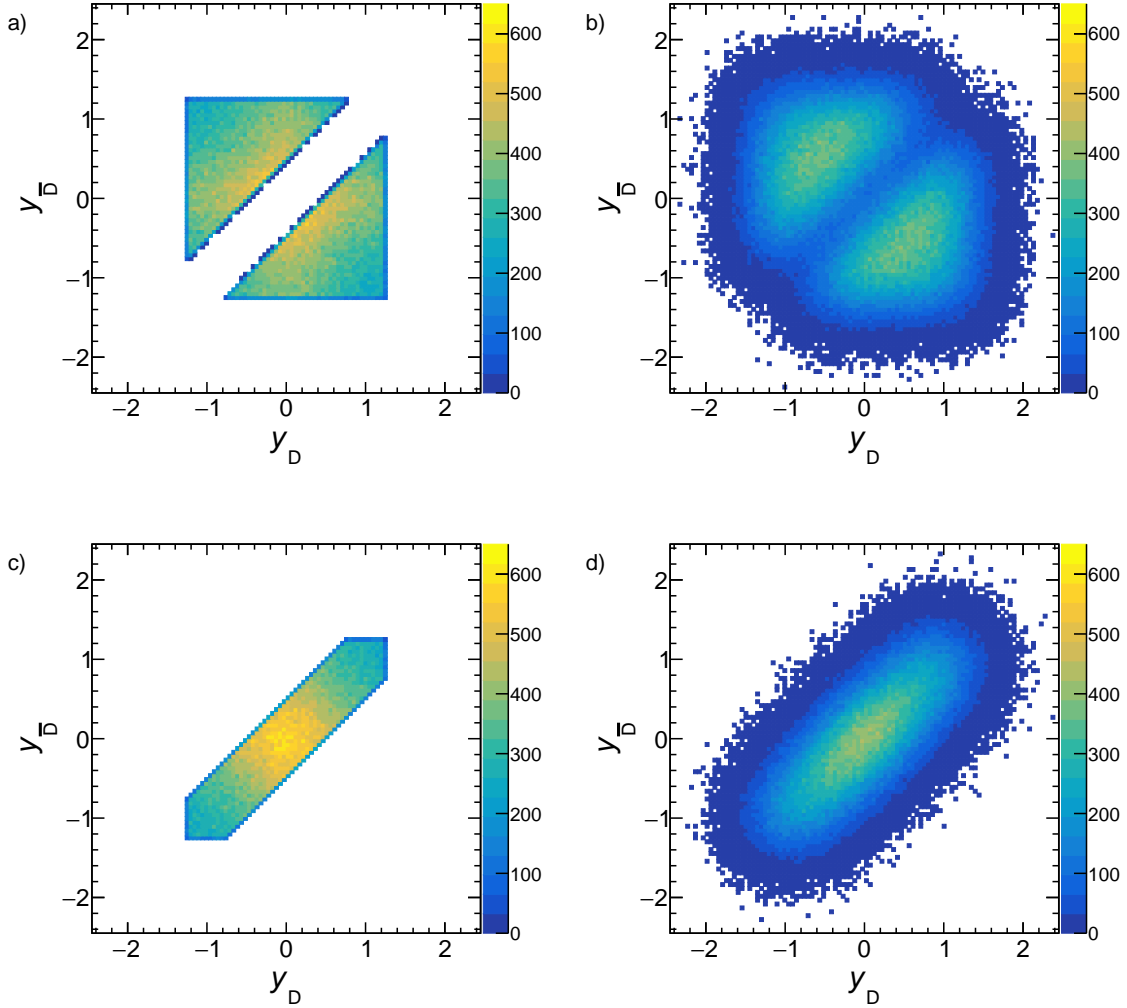


Figure 6: Joint rapidity distributions of D and \bar{D} mesons for the initial temperature $T_0 = 200$ MeV. The upper plots show the distributions for D and \bar{D} pairs, which can result only from the apparent teleportation. The lower plots show the results for the pairs, which can be attributed either to local-distinguishable processes or the apparent teleportation. The left plots are obtained without smearing due to statistical hadronisation, whereas the right ones include the smearing.

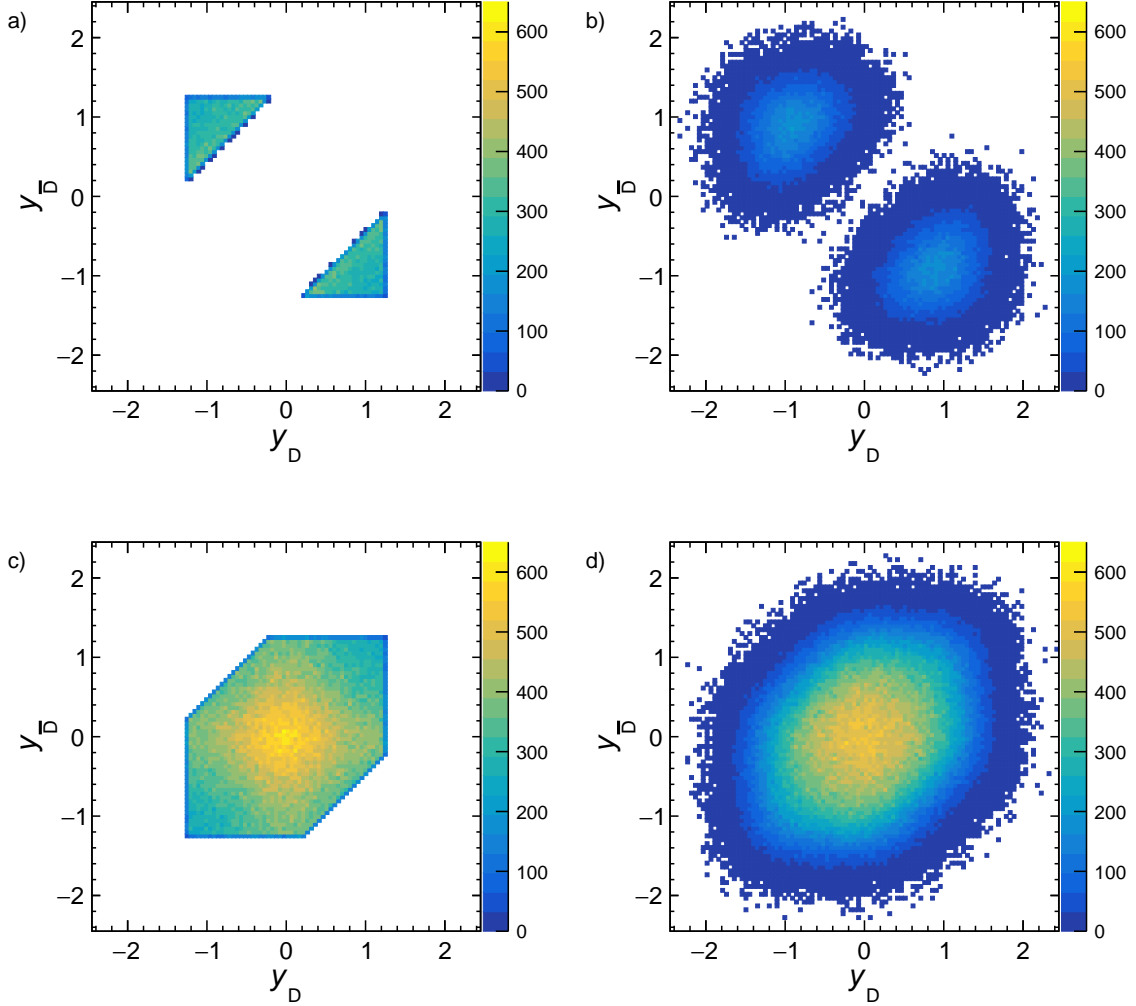


Figure 7: Joint rapidity distributions of D and \bar{D} mesons for the initial temperature $T_0 = 300$ MeV. The upper plots show the distributions for D and \bar{D} pairs, which can result only from the apparent teleportation. The lower plots show the results for the pairs, which can be attributed either to local-distinguishable processes or the apparent teleportation. The left plots are obtained without smearing due to statistical hadronisation, whereas the right ones include the smearing.

1+3D Blast-Wave model

A simple 1+3D model of high-energy nucleus-nucleus collisions with the properties necessary to investigate apparent teleportation is presented here. The model utilises the Blast-Wave model [30] of radial flow, which has been widely used for parametrising experimental results on hadron spectra for decades. For simplicity, only central Pb+Pb collisions are considered. The model assumptions are as follows.

- (i) The initial stage ($t = 0$) of the matter created in a central Pb+Pb collision is approximated as a sphere of radius $R = 6$ fm (the radius of the Pb nucleus), centred at the origin of the coordinate system. The density is assumed to be isotropic.
- (ii) The hadronisation state, where the radial flow stops, is approximated as a sphere with radius $2R$.
- (iii) The radial flow velocity at hadronisation at position $\mathbf{r} = (x, y, z)$ is given by:

$$\mathbf{v}(\mathbf{r}) = c \cdot \mathbf{r}/(2R) , \quad (8)$$

where c is set to one. The hadronisation occurs at time $t_{\text{HAD}} = R/v(r = 2R) = c/R$.

The distribution function of a pair of D and \bar{D} mesons generally depends on six momentum components (\mathbf{p}_D and $\mathbf{p}_{\bar{D}}$). However, due to the spherical symmetry of the model, this dependence reduces to three non-trivial momentum quantities. Here, we select them as:

- The opening angle between the momentum vectors, Θ , where $\Theta = |\theta_D - \theta_{\bar{D}}|$ and $\theta_D, \theta_{\bar{D}}$ are the polar angles of D, \bar{D} mesons changing in the range $[0, \pi]$.
- The momentum magnitudes p_D and $p_{\bar{D}}$.

The model predictions are as follows.

Neglecting the non-flow component of the final velocity, if the hadronisation points of c and \bar{c} are chosen independently, the opening angle Θ varies between 0 and π . The cosine of the opening angle, $\cos(\Theta)$, is uniformly distributed. This set of pairs includes both local-distinguishable pairs and those violating this condition.

At $t = 0$, the collision light cone is a sphere with radius R centred at $(0, 0, 0)$. Simultaneously, the past light cones of the hadronising c and \bar{c} quarks on a sphere with radius $r = aR$ ($0 \leq a \leq 2$) are also spheres of radius R , but centred at \mathbf{r}_c and $\mathbf{r}_{\bar{c}}$ ($r_c = r_{\bar{c}} = aR$), respectively.

The maximum allowed opening angle $\Theta_{\text{MAX}}(aR)$ for which the LD condition is obeyed is:

$$\Theta_{\text{MAX}}(aR) = 180^\circ - \cos^{-1}(1 - a^2/2) . \quad (9)$$

For $a = 2$ (the maximum hadronisation surface radius), $\Theta_{\text{MAX}} = 0$, while for $a \rightarrow 1$, $\Theta_{\text{MAX}} \rightarrow 120^\circ$. For $a = 1$ and below, $\Theta_{\text{MAX}} = 180^\circ$. A sketch illustrating this calculation is shown in Fig. 8.

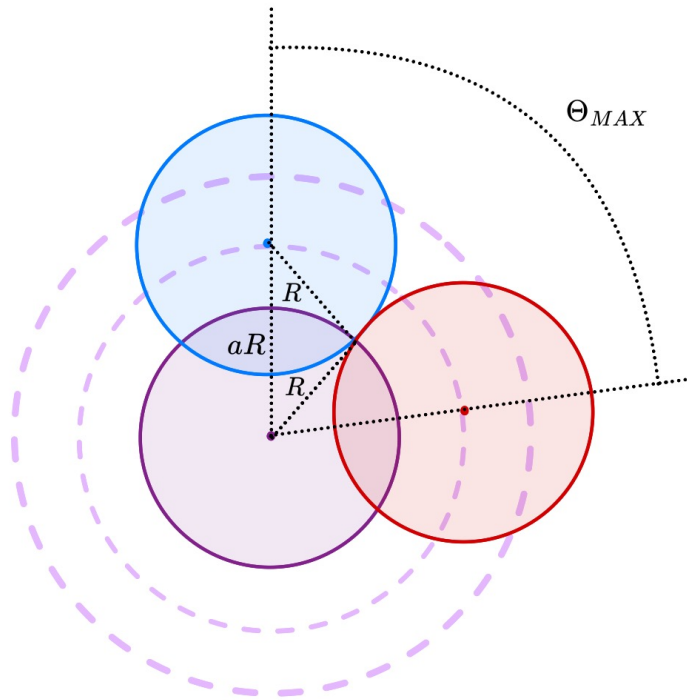


Figure 8: Sketch illustrating the calculation of the maximum possible opening angle Θ_{MAX} between the c and \bar{c} quarks hadronising at $r = a \cdot R$ and obeying the LD condition. The plot shows the intersection of the plane defined by the hadronisation points and the collision centre with the past light-cone spheres of the c (red) and \bar{c} quarks, as well as the collision light cone at $t = 0$. The angle Θ_{MAX} is determined by the requirement of a single common point of the three circles.

The LD condition suppresses the opening angle distribution at large angles, with the effect strongest for pairs emitted from $r = 2R$, where $\Theta_{\text{MAX}} = 0^\circ$. For pairs hadronising at small radii ($r \leq R$) one gets $\Theta_{\text{MAX}} = 180^\circ$.

To test for apparent teleportation, one can focus on pairs emitted from the outer hadronisation layer (high-momentum D and \bar{D} mesons). Observing pairs with $\Theta > \Theta_{\text{MAX}}$ at high momentum would indicate apparent teleportation of c and \bar{c} quarks.

ACKNOWLEDGMENTS

We are thankful to F. Giacosa, M. Gorenstein, D. Miskowicz and St. Mrowczyński for their comments. This work is partially supported by the Polish National Science Centre grants 2018/30/A/ST2/00226, 2018/30/E/ST2/00089 and 2020/39/D/ST2/02054.

-
- [1] M. Maku, *Teleportation and Science Fiction*. Random House Digital, 2008.
- [2] C. H. Bennett, G. Brassard, C. Crepeau, R. Jozsa, A. Peres, and W. K. Wootters, “Teleporting an unknown quantum state via dual classical and Einstein-Podolsky-Rosen channels,” *Phys. Rev. Lett.* **70** (1993) 1895–1899.
- [3] D. Bouwmeester, J.-W. Pan, K. Mattle, M. Eibl, H. Weinfurter, and A. Zeilinger, “Experimental quantum teleportation,” *Nature* **390** (1997) 575–579.
- [4] J. Yin *et al.*, “Satellite-based entanglement distribution over 1200 kilometers,” *Science* **356** no. 6343, (2017) aan3211.
- [5] W. Pfaff *et al.*, “Unconditional quantum teleportation between distant solid-state quantum bits,” *Science* **345** no. 6196, (2014) 532–535.
- [6] S. Pirandola, J. Eisert, C. Weedbrook, A. Furusawa, and S. L. Braunstein, “Advances in quantum teleportation,” *Nature Photon.* **9** (2015) 641–652.
- [7] M. A. Porrás, M. Casado-Álvarez, and I. Gonzalo, “Teleportation of a quantum particle in a potential via quantum Zeno dynamics,” *Phys. Rev. A* **109** no. 3, (2024) 032207, [arXiv:2305.07968](https://arxiv.org/abs/2305.07968) [quant-ph].
- [8] P. Facchi, V. Gorini, G. Marmo, S. Pascazio, and E. C. G. Sudarshan, “Quantum Zeno dynamics,” *Phys. Lett. A* **275** (2000) 12, [arXiv:quant-ph/0004040](https://arxiv.org/abs/quant-ph/0004040).
- [9] P. Facchi and S. Pascazio, “Quantum Zeno Subspaces,” *Phys. Rev. Lett.* **89** no. 8, (2002) 080401.
- [10] P. Facchi and S. Pascazio, “Quantum Zeno dynamics: mathematical and physical aspects,” *J. Phys. A* **41** no. 49, (2008) 493001.
- [11] An internally consistent model covering distinguishable and indistinguishable particles and antiparticles has to give identical predictions for a single particle or antiparticle in the system when treating it as distinguishable and indistinguishable.
- [12] M. Gazdzicki, M. Gorenstein, A. Fronczak, P. Fronczak, and M. Mackowiak-Pawłowska, “Steady state of isolated systems versus microcanonical ensemble in cell model of particle creation and annihilation,” *Int. J. Mod. Phys. E* **26** no. 12, (2017) 1750085, [arXiv:1704.01878](https://arxiv.org/abs/1704.01878) [nucl-th].

- [13] M. Gazdzicki, M. Gorenstein, I. Pidhurskyi, O. Savchuk, and L. Tinti, “Equilibration and Locality,” *Acta Phys. Polon. B* **53** no. 8, (2022) 2, [arXiv:2206.01151 \[nucl-th\]](#).
- [14] R. Hagedorn, “Statistical thermodynamics of strong interactions at high-energies,” *Nuovo Cim. Suppl.* **3** (1965) 147–186.
- [15] D. Miskowiec, “Quark-gluon plasma paradox,” *PoS CPOD07* (2007) 020, [arXiv:0707.0923 \[hep-ph\]](#).
- [16] W. Florkowski, *Phenomenology of Ultra-relativistic Heavy-ion Collisions*. World Scientific, 2010.
- [17] E. V. Shuryak, “Quantum Chromodynamics and the Theory of Superdense Matter,” *Phys. Rept.* **61** (1980) 71–158.
- [18] Y. Aoki, Z. Fodor, S. D. Katz, and K. K. Szabo, “The QCD transition temperature: Results with physical masses in the continuum limit,” *Phys. Lett. B* **643** (2006) 46–54, [arXiv:hep-lat/0609068](#).
- [19] **ALICE** Collaboration, B. Abelev *et al.*, “Centrality dependence of π , K, p production in Pb-Pb collisions at $\sqrt{s_{NN}} = 2.76$ TeV,” *Phys. Rev. C* **88** (2013) 044910, [arXiv:1303.0737 \[hep-ex\]](#).
- [20] **NA49** Collaboration, S. V. Afanasiev *et al.*, “Energy dependence of pion and kaon production in central Pb + Pb collisions,” *Phys. Rev. C* **66** (2002) 054902, [arXiv:nucl-ex/0205002](#).
- [21] **NA49** Collaboration, C. Alt *et al.*, “Pion and kaon production in central Pb + Pb collisions at 20-A and 30-A-GeV: Evidence for the onset of deconfinement,” *Phys. Rev. C* **77** (2008) 024903, [arXiv:0710.0118 \[nucl-ex\]](#).
- [22] M. Gazdzicki, M. Gorenstein, and P. Seyboth, “Onset of deconfinement in nucleus-nucleus collisions: Review for pedestrians and experts,” *Acta Phys. Polon. B* **42** (2011) 307–351, [arXiv:1006.1765 \[hep-ph\]](#).
- [23] E. Andronov, M. Kuich, and M. Gaździcki, “Diagram of High-Energy Nuclear Collisions †,” *Universe* **9** no. 2, (2023) 106, [arXiv:2205.06726 \[hep-ph\]](#).
- [24] M. Gazdzicki and M. I. Gorenstein, “On the early stage of nucleus-nucleus collisions,” *Acta Phys. Polon. B* **30** (1999) 2705, [arXiv:hep-ph/9803462](#).
- [25] **NA61/SHINE** Collaboration, A. Merzlaya, “First $D^0 + \bar{D}^0$ measurement in heavy-ion collisions at SPS energies with NA61/SHINE,” in *21st International Conference on Strangeness in Quark Matter 2024*. 10, 2024. [arXiv:2410.24014 \[nucl-ex\]](#).

- [26] M. Gazdzicki, D. Kikola, I. Pidhurskyi, and L. Tinti, “Production locality and spatial diffusion of heavy flavour at high energy densities,” [arXiv:2305.00212 \[hep-ph\]](#).
- [27] L. D. Landau, “On the multiparticle production in high-energy collisions,” *Izv. Akad. Nauk Ser. Fiz.* **17** (1953) 51–64.
- [28] R. Hagedorn and J. Rafelski, “Hot Hadronic Matter and Nuclear Collisions,” *Phys. Lett. B* **97** (1980) 136.
- [29] F. Becattini, J. Manninen, and M. Gazdzicki, “Energy and system size dependence of chemical freeze-out in relativistic nuclear collisions,” *Phys. Rev. C* **73** (2006) 044905, [arXiv:hep-ph/0511092](#).
- [30] E. Schnedermann, J. Sollfrank, and U. W. Heinz, “Thermal phenomenology of hadrons from 200-A/GeV S+S collisions,” *Phys. Rev. C* **48** (1993) 2462–2475, [arXiv:nucl-th/9307020](#).